Radiation-dominated particle and plasma dynamics

Radiation-dominated particle and plasma dynamics

Arkady Gonoskov[1,2,3] and Mattias Marklund[1]
[1]*Department of Physics, Chalmers University of Technology, SE–412 96 Göteborg, Sweden*
[2]*Institute of Applied Physics, Russian Academy of Sciences, Nizhny Novgorod 603950, Russia*
[3]*Lobachevsky State University of Nizhni Novgorod, Nizhny Novgorod 603950, Russia*

(Received 9 July 2018; accepted 31 August 2018; published online 19 September 2018)

We consider charged particle motion in a strong electromagnetic field of an arbitrary configuration and find a universal behaviour: for sufficient field strengths, the radiation losses lead to a general tendency of the charge to move along the direction that locally yields zero acceleration orthogonal to the direction of motion. This corresponds to the suppression of radiation losses according to both classical and quantum considerations. We show that such a radiation-free direction (RFD) exists at each point of an arbitrary electromagnetic field, while the time-scale of approaching this direction decreases with the increase in field strength. In the case of a sufficiently strong electromagnetic field, at each point of space, the charges mainly move and form currents along the local RFD, while the deviation of their motion from RFD can be calculated to determine their incoherent emission. This forms a general description of particle, and therefore plasma, dynamics in strong electromagnetic fields, the latter being generated by state-of-the-art lasers or in astrophysical environments.

https://doi.org/10.1063/1.5047799

I. INTRODUCTION

The development of state-of-the-art high-intensity laser systems has spurred renewed interest in radiation reaction and its effect on particle dynamics in strong electromagnetic fields.[1] The nature of radiation reaction has been a long-standing issue in the literature,[2–5] and the developments over the last decade have further clarified various aspects of this effect (for a review, see Refs. 2, 3, and 5–8). The fundamental structure of radiation reaction has been discussed in Refs. 9 and 10, the quantum nature of radiation reaction has been analyzed in, e.g., Refs. 11–18, while the effect of dissipation on electron motion has been considered in Refs. 19–25. The interest in this field has been further increased by the discovery of several somewhat counter-intuitive phenomena, such as straggling,[26,27] quenching,[28] radiation reaction trapping in traveling waves,[29] as well as normal (NRT)[30] and anomalous[31] radiative trapping (ART) in standing waves. Despite continuous efforts to develop analytical approaches,[20,22,24,32–34] the high degree of nonlinearity in many cases restricts the analysis to qualitative explanations, assisted by numerical simulations. General theoretical approaches can be useful for building a more comprehensive picture and developing experimental concepts at upcoming laser facilities.[35–38] Phenomena due to radiation reaction can be exploited for creating exotic sources of particles and radiation,[39–44] as well as extreme states of matter.[45,46]

In this paper, we demonstrate that a charged particle, moving in an arbitrary electromagnetic field, tends to move along a direction that locally yields zero lateral (orthogonal to the direction of motion) acceleration. The timescale at which this direction is approached decreases with increasing intensity. We derive an explicit expression for this direction, estimate the time-scale of approach, and present a general description of particle and plasma dynamics in strong fields, based on these findings.

II. THE RADIATION-FREE DIRECTION

Let us consider an arbitrary electromagnetic field and its effect on a charged particle at an arbitrary point of space and time. One may ask if there exists a direction of motion $\mathbf{n}$ for which the particle does not experience any lateral acceleration, i.e., $\mathbf{E} - (\mathbf{E}\cdot\mathbf{n})\mathbf{n} = -(v/c)(\mathbf{n}\times\mathbf{B})$, where v is the particle speed, c is the speed of light, and $\mathbf{E}$ ($\mathbf{B}$) is the local electric (magnetic) field vector. If a particle moves along such a direction with relativistic speed, the particle would predominantly not experience any radiation losses, since the lateral acceleration provides the dominant loss mechanism in both classical and quantum descriptions. We call this the *radiation-free direction* (RFD) and consider the problem of finding this direction in the generic case.

The problem can be formulated in an algebraic way by expressing the sought vector $\mathbf{n}$ through its coordinates in the orthogonal system of coordinates spanned by the vectors $\mathbf{B}$, $\mathbf{E} - (\mathbf{E}\cdot\mathbf{B})\mathbf{B}/B^2$ and $\mathbf{E}\times\mathbf{B}$ (if any of these vectors is equal to zero, the solution can be obtained under more specific and simple consideration). The statement of the problem then leads to a set of equations that can be solved and analyzed. However, to obtain some physical insights, we derive the solution using vector analysis. In order not to distract the reader, we postpone this analysis (see Sec. VI) and outline the conclusions that are crucial for further analysis.

For any local field vectors, there exists always exactly one radiation-free direction that depends continuously on $\mathbf{E}$ and $\mathbf{B}$ according to the expression

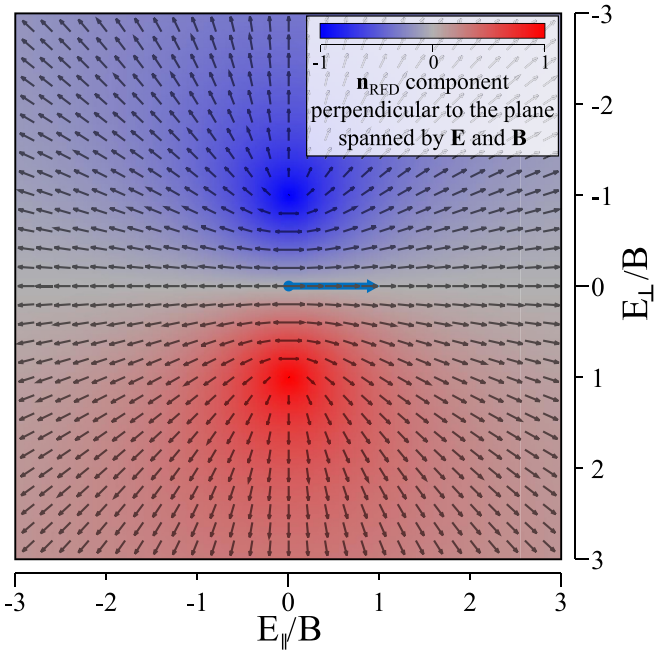

FIG. 1. Illustrating $\mathbf{n}^{+}_{\mathrm{RFD}}(\mathbf{E},\mathbf{B})$ by fixing $\mathbf{B}$ (blue arrow) and varying the end point of $\mathbf{E}$, keeping its starting point in the centre. For each position of the end point, the gray arrow shows the projection of $\mathbf{n}^{+}_{\mathrm{RFD}}$ on the plane spanned by $\mathbf{E}$ and $\mathbf{B}$, while the colour denotes the normal component.

$$\mathbf{n}^{\pm}_{\mathrm{RFD}} = \left\{\sqrt{u-u^2}(\mathbf{E}\times\mathbf{B}) \pm \left[(1-u)B\mathbf{E} + u(\mathbf{E}\cdot\mathbf{B})\mathbf{B}/B\right]\right\} \times \left[E^2B^2 - u(\mathbf{E}\times\mathbf{B})^2\right]^{-1/2}, \quad (1)$$

where the superscript denotes the sign of the charge and the value of u is given in the ultra-relativistic case by the expression (see Eq. (16) for the general case)

$$u = 2\frac{B^2}{E^2+B^2}\frac{1-\sqrt{1-w}}{w}, \quad w = \frac{4(\mathbf{E}\times\mathbf{B})^2}{(E^2+B^2)^2}. \quad (2)$$

The only exception is the case when $E<B$ and the $(\mathbf{E}\cdot\mathbf{B})$ changes the sign; in this case, $\mathbf{n}_{\mathrm{RFD}}$ changes discontinuously and the problem formally admits two solutions exactly at $(\mathbf{E}\cdot\mathbf{B})=0$. In order to show this, we provide the following graphical illustration (Fig. 1) of $\mathbf{n}_{\mathrm{RFD}}$ as the functional of vectors $\mathbf{E}$ and $\mathbf{B}$.

Since the result depends on the relative orientation of vectors $\mathbf{E}$ and $\mathbf{B}$, the functional (1) can be shown through varying the electric field components perpendicular $(E_\perp/B)$ and parallel $(E_\parallel/B)$ to the magnetic field vector $\mathbf{B}$. In Fig. 1, we present in such a way the view of $\mathbf{n}^{+}_{\mathrm{RFD}}$ (i.e., for positive charge), while $\mathbf{n}^{-}_{\mathrm{RFD}}$ can be obtained through inverting the component perpendicular to $\mathbf{E}\times\mathbf{B}$.

In Fig. 2, we demonstrate the correctness of the obtained result through direct computation of lateral acceleration for the case of $E_\parallel = B/2$.

III. APPROACHING THE RADIATION-FREE DIRECTION

Let us now discuss why the RFD plays an important role for understanding radiation-dominated dynamics. In this section, we show that intense radiation losses lead to a general tendency of charged particles to align their propagation directions along the local RFD, i.e., $\mathbf{n}^{\pm}_{\mathrm{RFD}}$ computed for local $\mathbf{E}$ and $\mathbf{B}$ vectors (see Fig. 3).

Radiation reaction gives a change of the particle's momentum, and this change is orientated almost exactly against the direction of propagation in the ultra-relativistic case. It is clear that this mismatch of the directions is not crucial for understanding the radiation-dominated dynamics, since, e.g., different radiation-induced trapping phenomena are observed in simulations under the assumption that the recoil from the radiation is always orientated exactly anti-parallel to the direction of propagation. Thus, radiation reaction itself cannot be directly responsible for the change of the direction of motion. Radiation reaction changes the

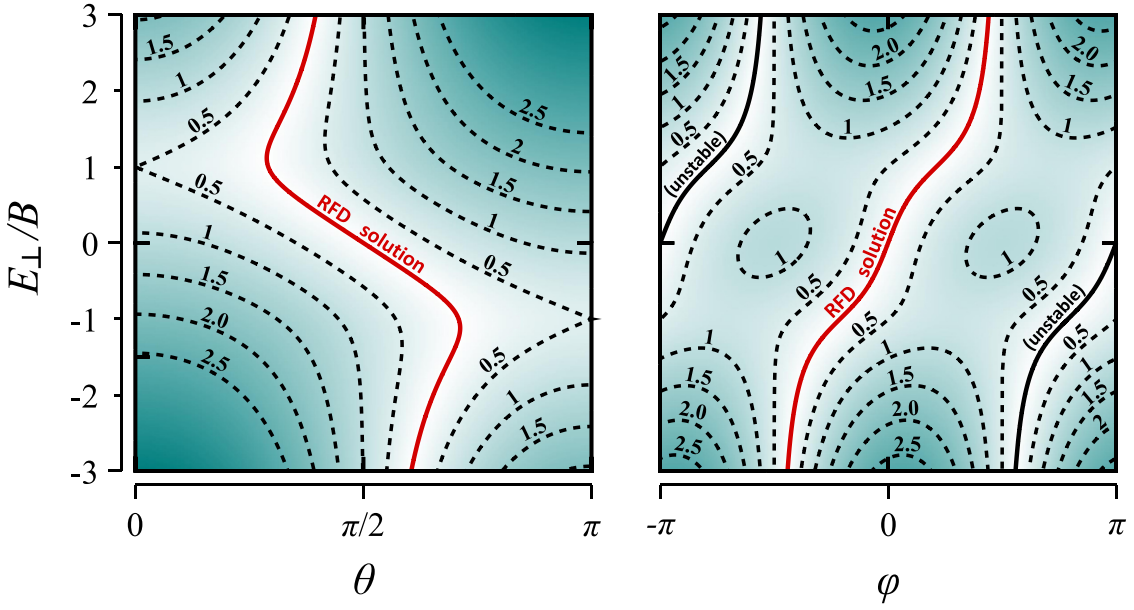

FIG. 2. Confirmation of the analytical results through a direct computation of the lateral acceleration for $E_\parallel/B = 1/2$, as a function of $E_\perp/B$. The amplitude of lateral acceleration (cyan shades) and the solution provided with the $\mathbf{n}^{+}_{\mathrm{RFD}}$ functional (red curves) are shown on the planes for varied polar angle θ (relative to the $\mathbf{E}\times\mathbf{B}$ direction) and azimuthal angle φ (relative to the $\mathbf{B}$ direction) of the direction of motion.

direction of propagation indirectly, through reducing the particle energy, so that the Lorentz force starts to affect the direction of propagation more strongly. We will now show that this results in approaching the RFD (1).

Suppose that a particle has the velocity $\mathbf{v}$, such that $\mathbf{v} = \mathbf{v}_{\mathrm{RFD}} + \Delta\mathbf{v}$, where $\mathbf{v}_{\mathrm{RFD}}$ is the radiation-free velocity and $\Delta\mathbf{v}$ is a small deviation thereof. The effects of radiation reaction can be discrete and stochastic, but for our analysis, it is sufficient to consider a continuous effect (we stress that our general result is valid independent of this choice of the radiation reaction treatment), where the radiation reaction force is given by $\mathbf{F}_{\mathrm{RR}} = -0.37m^2c\hbar^{-2}\chi^{2/3}\mathbf{v}$. This gives the averaged force in the limit of $\chi \gg 1$, where $\chi = \gamma F_\perp/E_{\mathrm{S}}$ is the quantum efficiency parameter for a particle experiencing a force of magnitude $F_\perp$ across its motion, and $E_{\mathrm{S}} = m^2c^3/\hbar$ is the Schwinger-Sauter field.[7] The equation for the evolution of the particles momentum $\mathbf{p}$ is

$$\frac{d}{dt}\mathbf{p} = \mathbf{E} + \frac{1}{c}(\mathbf{v}_{\mathrm{RFD}} + \Delta\mathbf{v}) \times \mathbf{B} + \mathbf{F}_{\mathrm{RR}} = \mathbf{e}_\parallel + \mathbf{F}_{\mathrm{RR}} + \frac{1}{c}\Delta\mathbf{v} \times \mathbf{b}_1 + \frac{1}{c}\Delta\mathbf{v} \times \mathbf{b}_2, \quad (3)$$

where the electric field $\mathbf{E}$ is decomposed into the sum of the parallel ($\mathbf{e}_\parallel$) and perpendicular ($\mathbf{e}_\perp$) components relative to the RFD, while the magnetic field $\mathbf{B}$ is decomposed into the sum of the component $\mathbf{b}_1$ lying in and $\mathbf{b}_2$ perpendicular to the plane spanned by $\mathbf{v}_{\mathrm{RFD}}$ and $\mathbf{v}$. The expression $(\mathbf{e}_\perp + \mathbf{v}_{\mathrm{RFD}} \times \mathbf{B}/c)$ is, by definition, identically zero and has been removed from the second line. We can now determine the effect of all four remaining terms in the sense of causing either approach to or deflection from the RFD. According to our treatment, the second term is parallel to $\mathbf{v}$ and thus gives no *direct* effect in this sense. Neither does the third term because it is perpendicular to the plane spanned by $\mathbf{v}_{\mathrm{RFD}}$ and $\mathbf{v}$. To determine the role of the first and the last terms, we can estimate the change of $\mathbf{v}$ in terms of $\partial(\Delta\mathrm{v})/\partial t$. We first note that in the relativistic limit $|\mathbf{v}| = |\mathbf{v}_{\mathrm{RFD}}| = c$, the angle between $\Delta\mathbf{v}$ and $\mathbf{v}$ (and also $\mathbf{v}_{\mathrm{RFD}}$) is $\phi = \arccos(\Delta\mathrm{v}/(2c)) \approx \pi/2$, and thus, it is close to $\pi/2$ also in the case of highly relativistic motion, which we are considering here. As one can see, both the first and last terms are almost parallel to the direction of motion. However, in terms of $\partial(\Delta\mathrm{v})/\partial t$, the first term provides the effect that is of the order of $[e_\parallel/(mc\gamma)]2\cos\phi \sim [e_\parallel/(mc\gamma)](\Delta\mathrm{v}/c)$, while the effect of the last term is $[b_2/(mc\gamma)]\ (\Delta\mathrm{v}/c)\cos\phi \sim [b_2/(mc\gamma)](\Delta\mathrm{v}/c)^2$. As we see, in terms of small $\Delta\mathbf{v}$, the last term gives the second order effect and thus the approach to or deviation from the

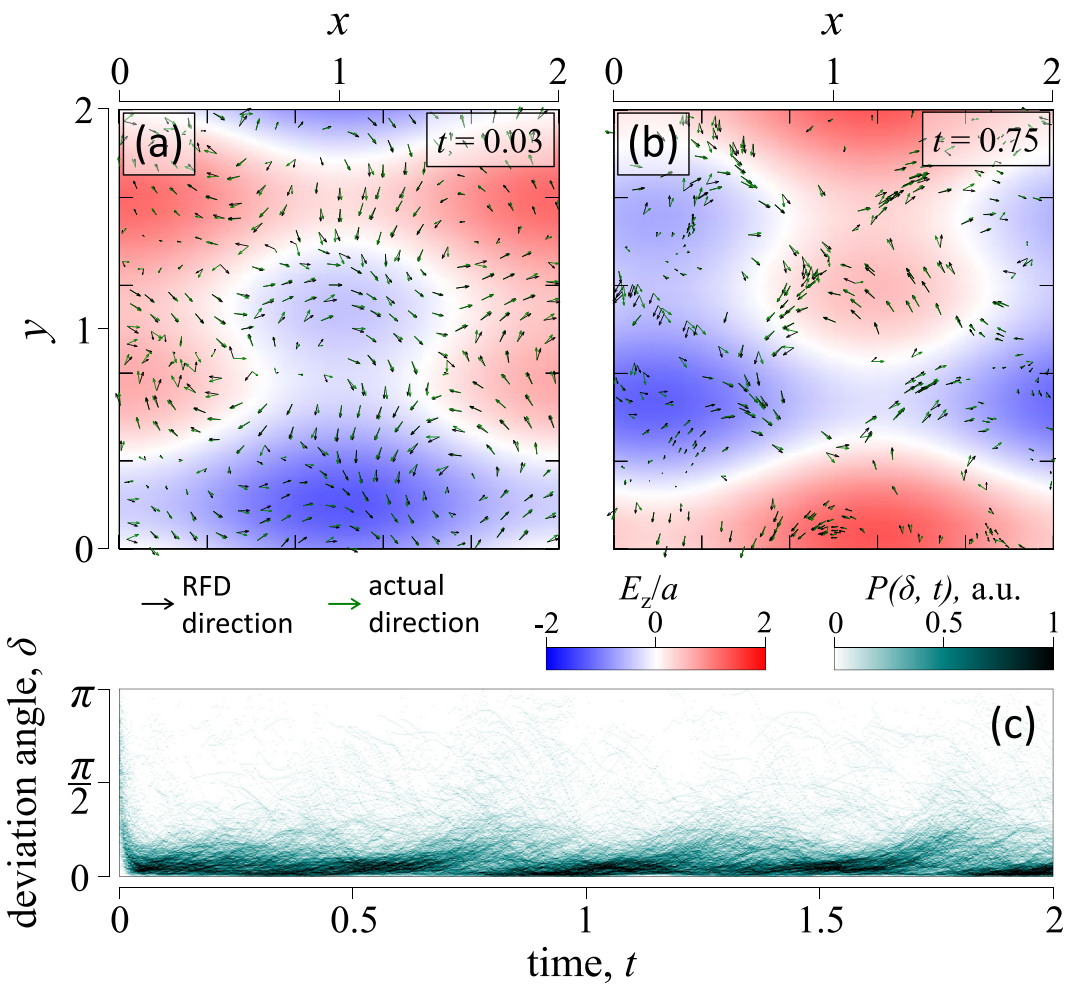

FIG. 3. The result of simulation of the particles' motion for the field amplitude $a = 10^4$. The position of particles is shown at (a) $t = 0.03$ and (b) $t = 0.75$. For each particle, we show the xy-projection of the direction of motion (green arrow) and of the RFD calculated for the local field (black arrow). The temporal evolution of particle distribution $P(\delta, t)$ in deviation angle δ is shown in (c). See supplementary video for the entire evolution. Multimedia view: https://doi.org/10.1063/1.5047799.1

radiation-free direction is governed by the electric field component parallel to the RFD, i.e., $\mathbf{e}_\parallel$.

Of two counter-orientated directions that yield zero lateral acceleration, the RFD direction (1) is defined so that $\mathbf{e}_\parallel$ points towards the radiation-free motion, making $\Delta\mathbf{v}$ smaller [with exceptions of $(E=0)$ and $(E=B, \mathbf{E}\perp\mathbf{B})$]. Thus, the force of $\mathbf{e}_\parallel$ acts so that a particle approaches the radiation-free direction. In fact, even if $\Delta\mathbf{v}$ is not small, the approach to the RFD can be understood as follows. The motion along the RFD is upheld by the electric field, while the motion in the transverse direction gets exhausted by radiation losses in an irreplaceable way.

In order to obtain the time-scale of this behaviour, we rewrite Eq. (3) in terms of the relativistic γ factor and the angle δ of deviation from the RFD. We obtain

$$\begin{aligned} mc\frac{d\gamma}{dt} &= e_\parallel \cos\delta - A\left(\gamma e_\parallel \sin\delta\right)^{2/3}, \\ mc\gamma\frac{d\delta}{dt} &= -e_\parallel \sin\delta, \end{aligned} \tag{4}$$

where $e_\parallel = |\mathbf{e}_\parallel|$ and $A = 0.37\alpha E_S^{1/3}$, $\alpha \approx 1/137$ is the fine-structure constant hereafter. Here, we used the rate of radiation losses in the limit of strong fields computed in the framework of quantum electrodynamics (QED). The system (4) is an autonomous system of differential equations, which is accessible for the analytical study via its phase plane. However, the crucial features and estimates can be obtained with the following simple analysis. First, we assume that $\delta \ll 1$. From the first equation of (4), we see that the particle can gain energy until the Lorentz force (the first term) becomes balanced by the radiation reaction (the second term). The smaller the deviation is, the higher the values of γ can be achieved. The limiting case of balance between these terms corresponds to the radiation-dominated regime.[47,48] For this limit, we can determine the relation

$$\gamma^{-1} \approx \delta A^{3/2} e_\parallel^{-1/2}. \tag{5}$$

Using the second equation in (4), we obtain

$$\frac{d}{dt}\delta = -\delta^2/\tau_{\mathrm{RFD}}, \tag{6}$$

where τ_{RFD}, the typical time-scale of approaching to the radiation-free direction, is given by

$$\tau_{\mathrm{RFD}} = (0.37\alpha)^{-3/2}\frac{mc}{e(e_\parallel E_S)^{1/2}} \approx 7100\frac{mc}{e(e_\parallel E_S)^{1/2}}, \tag{7}$$

where e is the charge of the positron. As one can see from Eq. (6), the particle indeed approaches the RFD ($\delta = 0$), with temporal evolution

$$\delta(t) \sim \tau_{\mathrm{RFD}}/t. \tag{8}$$

For the upcoming high-intensity lasers with an expected peak intensity of about 10^{23} W/cm^2, the estimate (7) gives $\tau_{\mathrm{RFD}} \approx 0.3$ fs, which is 10 times less than the wave period of laser radiation. This means that the tendency discussed here can play a significant role in the upcoming experiments.

During the particle motion, the RFD changes because of the time-dependence of the electromagnetic fields experienced by the particle. Assuming that the RFD changes with a typical frequency ω of the electromagnetic field, we can determine the typical value of the deviation angle as a function of the field amplitude a given in relativistic units $(mc\omega/e)$

$$\langle\delta\rangle \sim 7100/\sqrt{aa_S}, \tag{9}$$

where $a_S = mc^2/\hbar\omega$ is the Schwinger-Sauter field given in relativistic units relative to the frequency ω.

If we consider $\langle\delta\rangle < \pi/8$ as the criterion for the effect to appear in a prominent way, the amplitude necessary for this and the corresponding value of χ can be estimated as

$$a_{\mathrm{RFD}} \approx 3\times 10^8 a_S^{-1}, \quad \chi_{\mathrm{RFD}} \approx 10^{17} a_S^{-3}, \tag{10}$$

where we estimated $\gamma \approx a$ from Eq. (5). For high-intensity lasers (wavelength $\lambda = 1\,\mu$m, $\hbar\omega \approx 1.24\,$eV, $a_S \approx 0.4\times 10^6$), we estimate $a_{\mathrm{RFD}} \approx 10^3$ and $\chi_{\mathrm{RFD}} \gtrsim 1$, which motivates the use of expression for the radiation losses in the high χ range.

However, since $\chi_{\mathrm{RFD}} \sim \omega^3$, for larger wavelengths and, in particular, in astrophysical environments, the amplitude necessary for the appearance of radiation-dominated dynamics can be achieved for $\chi_{\mathrm{RFD}} \ll 1$, i.e., without the prominent role of pair production and other strong-field QED phenomena. We can perform the same analysis for the radiation losses in the classical form (for $\chi \ll 1$) $\mathbf{F}_{\mathrm{RR}}^{cl} = -(2/3)m^2c\hbar^{-2}\chi^2\mathbf{v}$. In this case, we can again obtain Eqs. (6) and (8) but with

$$\tau_{\mathrm{RFD}}^{cl} \approx 14\frac{mc}{ee_\parallel^{3/2}E_S^{-1/2}}. \tag{11}$$

Using this, we can obtain the following estimates:

$$a_{\mathrm{RFD}}^{cl} \approx 10 a_S^{1/3}, \quad \chi_{\mathrm{RFD}}^{cl} \approx 100 a_S^{-1/3}. \tag{12}$$

As we can see, these estimates can also be relevant for high-intensity lasers. However, the obtained estimates are still rough, since we, for example, do not account for the time-scale of reaching the assumed balance between the Lorentz force and the radiation reaction [Eq. (4)]. Our main intention here was to show the origin of the effect and obtain some typical scales, while some more precise results are presented and discussed in Sec. V on the basis on numerical simulations.

We also would like to note that the assumed here *continuous* form of radiation reaction is not crucial for understanding the mechanism and performing the estimates. Indeed, losing momentum in discreet portions still has the same effect of making the particle relativistically "lighter" and thus more sensitive for the change in the direction by the Lorentz force. After each emission, the particle is re-accelerated more towards the RFD than in other directions. Although the approach to the RFD appears as a robust phenomenon, the discreetness and stochasticity of emission can lead to spreading of the distributions relative to classical results and cause other effects.[12,13,18] We discuss some effects of this type also in Sec. V.

IV. OCCURRENCE OF RADIATION-FREE MOTION

A. Anomalous radiative trapping

One consequence of radiation-free motion is the phenomenon of anomalous radiative trapping (ART).[31] The

explanation given in Ref. 31 is based on the emergence of radiation-free motion for linearly polarized electromagnetic standing waves (see Fig. 1(c) in Ref. 31). Here, we can estimate the threshold amplitude $a_{\text{th}}^{\text{ART}}$ for this effect, using Eq. (7). In order for particles to migrate from the vicinity of an electric field node [where the particles are accumulated by normal radiation trapping (NRT)], the radiation-dominated motion should appear in a small (enough) neighborhood around this point. According to Fig. 1(c) in Ref. 31, the typical spread of particles around the magnetic field node in the NRT regime is about 1/10 of the wavelength and the typical electric field strength at this point is about 1/10 of the standing-wave amplitude. Therefore, radiation-free motion can dominate the particle dynamics if, e.g., τ_{RFD} is less than one eighth of the wave period. Equation (7) then yields $a_{\text{th}}^{\text{ART}} \approx 2000$ (in relativistic units), which is fully consistent with the threshold determined numerically in Ref. 31 (see Fig. 1(a) of that reference).

B. Radiation reaction trapping

The phenomenon of radiation reaction trapping[29] is another case that can be explained within the current framework. For radiation reaction trapping, particles tend to co-propagate with an intense laser pulse. From the analysis presented here, we see that the role of the radiation reaction is to reduce the gamma factor of the electrons so that the Lorentz force can quickly deflect the particles towards the RFD. It is straightforward to see that for the case of a traveling plane wave with the electric and magnetic fields equal and perpendicular to each other, the radiation-free direction coincides with the wave vector or the direction of laser pulse propagation (see Fig. 1). Once the particles come close to this direction, they can propagate for a long time together with the pulse. However, since in this case the electric field vector is orientated perpendicular to the radiation-free direction, the estimate of the typical time of approaching this direction requires further analysis of Eq. (3). Note that the problem of particle motion in a plane wave admits an exact analytical solution.[23] However, the general tendency of particles towards the co-motion with the plane wave in the case of strong losses is known from the following qualitative argument.[2] Since the particles receive energy through absorbing momentum exactly in the wave vector direction but lose the energy through emitting photons in various directions, the energy balance gradually leads to the motion along the wave vector. As a simple particular example for the RFD tendency, this known behavior supports our conclusions.

C. Plasma dynamics

For sufficiently strong fields, the convergence (8) to the RFD can be faster than the typical timescale of the field. In this case, particles will follow the local RFD at each point of spacetime, creating currents that in turn will affect the electromagnetic fields. Using this as a key assumption, we can obtain a self-consistent description of such radiation-dominated plasma dynamics in the form

$$\partial f_i + c\mathbf{n}_{\text{RFD}}^{\pm}(\mathbf{E},\mathbf{B}) \cdot \nabla f_i = 0, \tag{13}$$

$$\partial f_k + \mathbf{v}_k \cdot \nabla f_k + q_k \left(\mathbf{E} + \frac{\mathbf{v}_k}{c} \times \mathbf{B} \right) \cdot \frac{\partial f_k}{\partial \mathbf{p}_k} = 0, \tag{14}$$

with $\rho = \sum_k q_k \int f_k d^3p + \sum_i q_i f_i$ and $\mathbf{j} = \sum_k q_k \int f_k \mathbf{v}_k d^3p + \sum_i q_i f_i c \mathbf{n}_{\text{RFD}}^{\pm}(\mathbf{E},\mathbf{B})$ being the charge density and current density, respectively, and the particle velocity given by $\mathbf{v}_k = \mathbf{p}_k [1 + \mathbf{p}_k^2/(m_k c)^2]^{-1/2}/m_k$. Here, the index i denotes particles that undergo radiation-free motion and k denotes other particles (for example, heavier ions), f_i and f_k are the respective distribution functions, and the self-consistent fields are governed by Maxwell's equations with the currents and charge densities generated by the above distribution functions. Note that this description does not imply the absence of radiation, which can be obtained through the evolution of RFD and the gamma factor across the obtained trajectories. This description can also be extended by accounting for the related particles' redistribution between the radiation-free trajectories (as a second order effect).

V. NUMERICAL BENCHMARKING

We analyze our analytical approach and identify its range of applicability, by performing simulations of the exact equations of motion. We considered an array of positrons moving in an arbitrary chosen configuration of the electromagnetic field that has a typical frequency ω and amplitude a in relativistic units. For this purpose, we consider eight linearly polarized plane waves each having the frequency of ω or $\omega/2$ and propagating in a positive or negative direction of the x or y axis of a right-handed coordinate system $\{x, y, z\}$. The waves have arbitrarily chosen phases and polarization and arbitrarily chosen amplitudes with the average value of $0.475a$. We use dimensionless time t and coordinates x and y, normalized by the period $T = 2\pi/\omega$ and wavelength $\lambda = 1\ \mu$m, respectively.

The field structure is uniform along z and has a period of 2 along both the x and y directions. Initially, the positrons have random momenta of typical scale mca and are placed equidistantly within this periodic region. We employ periodic boundary conditions during their motion, computed in the given field. Radiation reaction is accounted for through photon emission events according to the QED rate expressions as it is described in Ref. 8. We present the result of our simulation for the case of $a = 10^4$ in Fig. 3. One can clearly see that within a period of time of about $0.05T$, the particles on average start to move along the RFD, and after that, the deviation angle remains small on average, i.e., the directions of particle motion (green arrows) systematically approach the local RFD (black arrows).

During the motion of a particle, the local fields change smoothly in time and so does RFD most of the time. However, if $E_{\parallel}$ changes sign and $E_{\perp} < B$, the RFD changes suddenly (see Fig. 1). (This explains the large deviations observable for some particles in Fig. 3.) We can thus distinguish two qualitatively different regimes of motion and emission: the regime of smooth evolution of the RFD and the regime of sudden change of the RFD. In the former case, the lateral acceleration is determined by the speed of RFD rotation during the particle motion. In this regime, the deviation angle remains small and this results in a moderate lateral

acceleration and the emission of photons under relatively small values of χ. Thus, in this regime, a particle continuously gains energy and emits it predominantly in the form of relatively low-energy photons. In the latter case, the deviation angle and the lateral acceleration instantaneously become large and this results in the emission of high-energy photons with large values of χ. In this case, a particle can emit a significant portion of the gained energy in the form of a single photon. The effect of radiation quenching[28] can delay this event, but after the emission of photons, the particle starts to emit more frequently and again follow the motion along the RFD.

The case of $E_{\parallel} \equiv 0$ deserves a separate consideration as it corresponds to both a linearly polarized standing wave and a dipole wave, which both can enable the ART effect.[31] In this case, $(\mathbf{E} \cdot \mathbf{B}) = 0$ is maintained during the motion, while the regimes of $E > B$ and $E < B$ appear one after another. A brief analysis of the particles' dynamics and the way it leads to the appearance of the ART phenomenon as a consequence of the tendency to the RFD is discussed in Ref. 31; a more detailed analysis can be found in Ref. 34. Note that during the particle motion in the ART regime, $E_{\perp}$ becomes less than B and the particles enter the bifurcation regime (see Fig. 1). If a particle continues the motion perpendicular to $\mathbf{B}$ (since the Lorentz force points along this plane), the particle starts to move having a large deviation angle and thus significant lateral acceleration. This means that the emission happens under large values of χ, which favors the emission of high-energy photons. This underlies the efficiency of the concept proposed for the generation of GeV photons at the upcoming laser facilities based on the ART dynamics in a dipole wave.[43] In this paper, the total power of a laser facility was varied in the range from 7 to 40 PW, and for the considered field configuration, this corresponds to the peak field amplitudes in the range from $a \approx 2000$ to $a \approx 5000$. This means that the approach suggested here can be useful for theoretical studies related to upcoming high-intensity laser facilities.[35–38]

To identify the applicability of the proposed approach for different field strengths, we perform the described simulations for a range of values of the amplitude a, and for each case, we determine the average deviation angle $\langle\delta\rangle$ for the second half of the simulation. The result of this study is shown in Fig. 4 together with the estimate (9). Although one can see a reasonable agreement, the expression (9) systematically underestimates the typical deviation angle. One reason for this is the fact that when obtaining the expression (9), we do not account for the regime of deviation from RFD during its sudden change. However, it is important that the estimate (9) reproduces the general tendency and thus explains the origin of the observed dynamics. For the physics of high-intensity laser-plasma interactions (see scales for $\lambda = 1\ \mu$m), a systematic approach of the particles to the RFD appears at intensities $\sim 10^{23}$ W/cm^2. This becomes dominating for intensities above 10^{25} W/cm^2, which are expected to be reached at the large-scale high-intensity laser facilities of the next generation. Note that at high field strengths, the effects of strong-field QED can take place. In this case, the tendency of particles to move along the RFD can still provide useful insights, while, for example, the effect of pair production can be included as a source term in Eq. (13).

VI. GEOMETRICAL DERIVATION OF THE RADIATION-FREE DIRECTION

In this section, we rigorously demonstrate the existence of RFD for the arbitrary case and derive the explicit expression for the $\mathbf{n}^{\pm}_{\mathrm{RFD}}(\mathbf{E}, \mathbf{B})$ functional. As we mentioned in Sec. II, the problem statement is to find the direction that yields zero lateral acceleration, i.e., $\mathbf{E} - (\mathbf{E} \cdot \mathbf{n})\mathbf{n} + (v/c)\,(\mathbf{n} \times \mathbf{B}) = 0$.

Let $\mathbf{P}$ be an arbitrary point in a three dimensional space for vectors $\mathbf{E}$ and $\mathbf{B}$ and consider a sphere with the centre in the point $\mathbf{P} + (1/2)\mathbf{E}$ and the radius $|\mathbf{E}|/2$ [see Fig. 5(a)]. We associate each point $\mathbf{D}$ of this sphere with the direction of propagation orientated along the vector $\mathbf{d} = \mathbf{D} - \mathbf{P}$. We now define a point $\mathbf{G} = \mathbf{P} + \mathbf{E}$. The vector $\mathbf{F}^{E}_{\perp} = \mathbf{D} - \mathbf{G}$ is

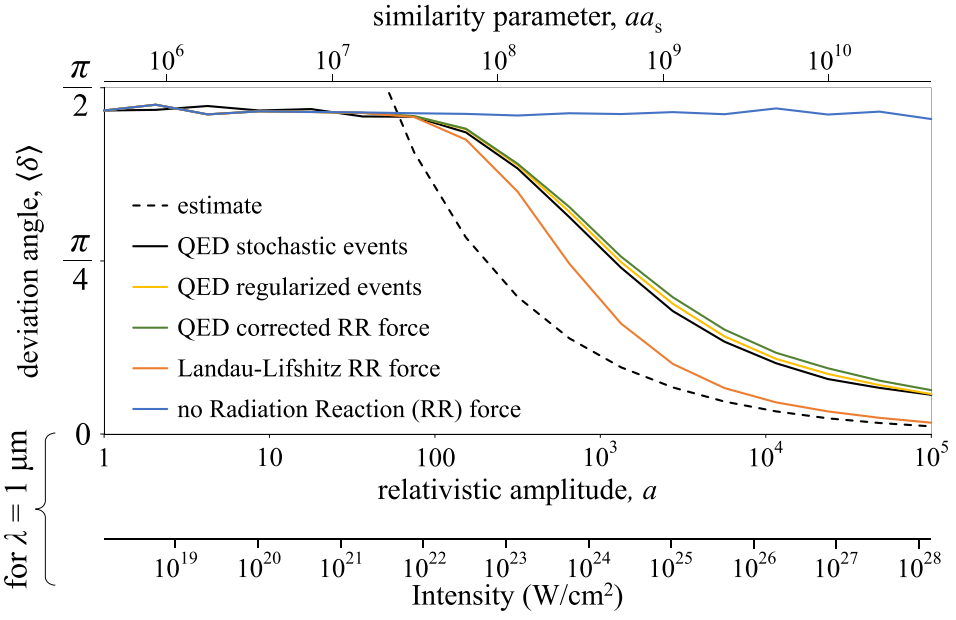

FIG. 4. The dependency of the average deviation angle $\langle\delta\rangle$ on the field amplitude in relativistic units. The results obtained numerically with different models for the radiation reaction are shown with solid curves (see the description in the diagram), and the result of the estimate (9) is shown with a dashed curve.

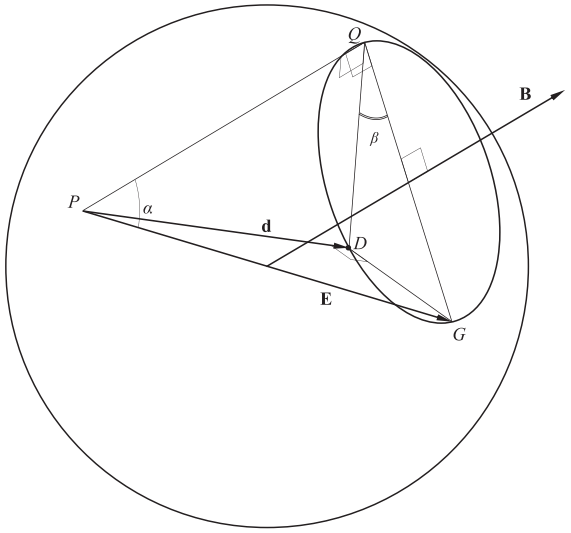

FIG. 5. The general setup of the vectors defined in the text.

then the transverse component, relative to the particle direction of motion, of the Lorentz force due to the electric field (for simplicity, we assume the charge to be equal to unity here).

The magnetic part of the Lorentz force $\mathbf{F}^B$ is always perpendicular to the magnetic field vector $\mathbf{B}$ and the direction of the particle motion. The transverse component $\mathbf{F}^B_\perp$ thus coincides with $\mathbf{F}^B$. In order for $\mathbf{F}^B_\perp$ to cancel $\mathbf{F}^E_\perp$, the latter has to be perpendicular to the magnetic field vector. We are therefore restricted to consider directions corresponding to a point on the circle formed by the intersection of the sphere with the plane passing through the point $\mathbf{G}$, being perpendicular to $\mathbf{B}$. For all points of this circle, $\mathbf{F}^E_\perp \perp \mathbf{B}$ holds. Moreover, on this circle, $\mathbf{F}^B_\perp$ and $\mathbf{F}^E_\perp$ are also parallel to each other. (The only exception is the case of the vector $\mathbf{d}$ being parallel to the vector $\mathbf{B}$, which results in $\mathbf{F}^B_\perp = 0$, thus not contradicting the final conclusions of this section). Indeed, if the vectors $\mathbf{d}$ and $\mathbf{B}$ are not parallel, then for the planes perpendicular to these vectors and passing through the point $\mathbf{D}$, there is a single line of intersection. Both $\mathbf{F}^B_\perp$ and $\mathbf{F}^E_\perp$ have to be parallel to this line, as each of them lies in both planes. Thus, $\mathbf{F}^B_\perp$ and $\mathbf{F}^E_\perp$ are parallel to each other.

As a result, in order for the particle to have zero lateral acceleration, we only need to request that $|\mathbf{F}^B_\perp| = |\mathbf{F}^E_\perp|$ (as will be shown, one of the solutions of this equation corresponds to the opposite orientations of the vectors, thus cancelling each other).

Let us consider a point $\mathbf{Q}$, which belongs to the circle and is opposite to the point $\mathbf{G}$. The segment $\mathbf{PQ}$ is parallel to $\mathbf{B}$. We define α as the angle between $\mathbf{E}$ and $\mathbf{B}$. The length of the $\mathbf{QG}$ segment is then $|\mathbf{QG}| = E\sin\alpha$. We define β as the angle between segments $\mathbf{QG}$ and $\mathbf{QD}$. The value of $\beta \in [-\pi/2, \pi/2]$ defines the position of the point $\mathbf{D}$ on the circle. Thus, $|\mathbf{F}^E_\perp| = |\mathbf{DG}| = E\sin\alpha|\sin\beta|$.

Suppose $\mathbf{v}$ is the particle's velocity vector, and $\mathbf{v}_\perp$ is its component across the vector $\mathbf{B}$. Then, the ratio $|\mathbf{v}_\perp|/|\mathbf{v}| = v_\perp/v$ is equal to the ratio of the lengths of the segment $\mathbf{QD}$ to the one of the segment $\mathbf{PD}$ in the right-angled triangle $\mathbf{PQD}$. As a result, we obtain

$$|\mathbf{F}^B_\perp| = \frac{v_\perp}{c}B = \frac{v}{c}\frac{B\sin\alpha\cos\beta}{\sqrt{\cos^2\alpha + \sin^2\alpha\cos^2\beta}}. \quad (15)$$

Equating $|\mathbf{F}^B_\perp|$ and $|\mathbf{F}^E_\perp|$, we obtain the equation $u^2\sin^2\alpha = u(k+1) - k$ for the unknown quantity $u = \sin^2\beta$, where $k = (v/c)^2(B/E)^2$. One can show that in the range $0 < u < 1$, this equation always only has the solution

$$u = \frac{(k^{1/2} + k^{-1/2}) - \left[(k^{1/2} + k^{-1/2})^2 - 4\sin^2\alpha\right]^{1/2}}{2k^{-1/2}\sin^2\alpha}. \quad (16)$$

Assuming $v \approx c$ and using $(\mathbf{E}\times\mathbf{B})^2 = E^2B^2\sin^2\alpha$, we have in the ultra-relativistic case

$$u = 2\frac{B^2}{E^2+B^2}\frac{1-\sqrt{1-w}}{w}, \quad w = \frac{4(\mathbf{E}\times\mathbf{B})^2}{(E^2+B^2)^2}. \quad (17)$$

As one can see, the maximal value of w is unity and thus u is always real. For each u, there are two values of β that give $\sin^2\beta = u$. One of these corresponds to the case of the opposite orientation of the electric and magnetic components, cancelling each other. Using the geometry of Fig. 5(a), we derive the expression (1) presented in the beginning of the article.

VII. CONCLUSIONS

In this paper, we have analysed particle motion in the limit of strong radiation reaction. We have shown that for arbitrary electric and magnetic fields, there is always one direction of propagation that leads to the absence of lateral acceleration. We also demonstrate that the particles approach this direction within a finite, characteristic time, and we derive expressions for the representative dynamics of this approach towards the radiation-free direction. We discuss how our conclusions can provide a possibility to analyze and understand particle and plasma dynamics in strong fields.

ACKNOWLEDGMENTS

We thank Tom Blackburn and Anton Ilderton for helpful and stimulating discussions. This research was partly supported by the Russian Science Foundation Project No. 16-12-10486 (A.G., computations), by the Swedish Research Council Grant Nos. 2013-4248, 2016-03329 (M.M.), and 2017-05148 (A.G.), and by the Knut & Alice Wallenberg Foundations. The simulations were performed on resources provided by the Swedish National Infrastructure for Computing (SNIC) at HPC2N.

[1]I. C. E. Turcu, F. Negoita, D. A. Jaroszynski, P. Mckenna, S. Balascuta, D. Ursescu, I. Dancus, M. O. Cernaianu, M. V. Tataru, P. Ghenuche, D. Stutman, A. Boianu, M. Risca, M. Toma, C. Petcu, G. Acbas, S. R. Yoffe, A. Noble, B. Ersfeld, E. Brunetti, R. Capdessus, C. Murphy, C. P. Ridgers, D. Neely, S. P. D. Mangles, R. J. Gray, A. G. R. Thomas, J. G. Kirk, A. Ilderton, M. Marklund, D. F. Gordon, B. Hafizi, D. Kaganovich, J. P. Palastro, E. D'Humieres, M. Zepf, G. Sarri, H. Gies, F. Karbstein, J. Schreiber, G. G. Paulus, B. Dromey, C. Harvey, A. Di Piazza, C. H. Keitel, M. C. Kaluza, S. Gales, and N. V. Zamfir, "High field physics and QED experiments at ELI-NP," Rom. Rep. Phys. **68**, 145 (2016).

[2]Ya. B. Zel'dovich, "Interaction of free electrons with electromagnetic radiation," Sov. Phys. Usp. **18**, 79 (1975).